ADVANCED X-RAY IMAGING TECHNIQUES FOR NON-DESTRUCTIVE ANALYSIS OF FUSION MATERIALS

I. Tiseanu , T. Craciunescu and team

EURATOM-MEdC, National Institute for Lasers, Plasma and Radiation Physics NILPRP, Bucharest, Romania

http://tomography.inflpr.ro

e-mail: tiseanu@infim.ro

ASSOCIATION DAYS MEETING, IASI, July, 2010

INFLPR experience in X-ray microCT for NDT inspection of fusion materials

X-RAY MICROTOMOGRAPHY for IFMIF

- IFMIF HFTM miniaturized specimens and irradiation capsule

X-RAY MICROTOMOGRAPHY for JET/ITER

- ITER- Compressed pebble bed
- ITER- Welded Steel Pipe with Cu cables
- ITER like Nb3Sn superconducting wires
- MgB2 superconducting wires
- JET reference CFC material NB31
- NDT inspection of tungsten coating uniformity
- NDT inspection of CFC / Cu/CuCrZr interfaces

http://tomography.inflpr.ro

UPGRADED: INFLPR X-RAY nano-CT FACILITY

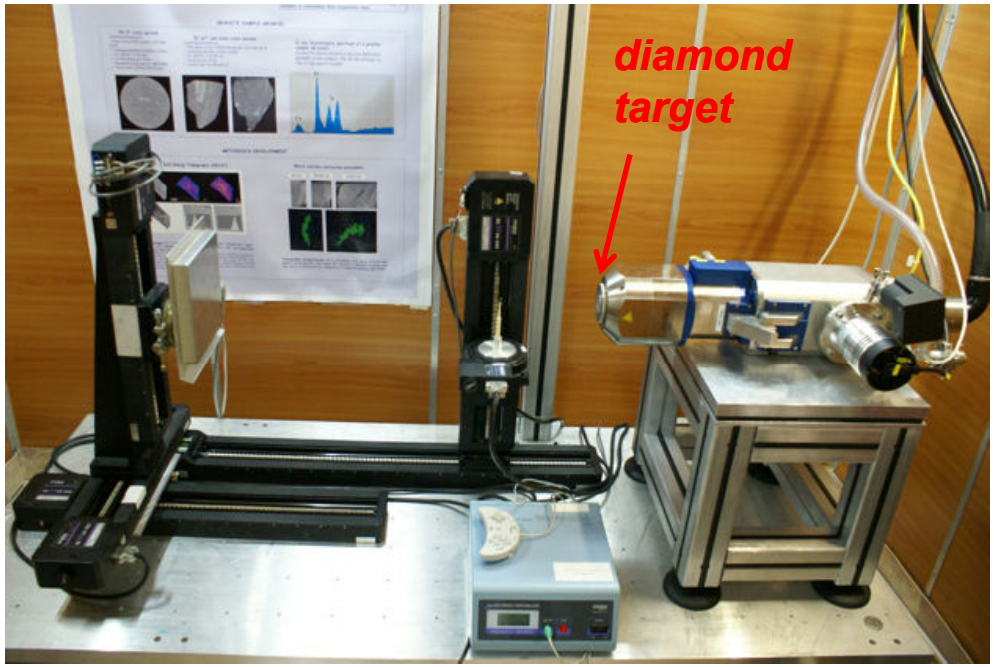

Recently, the X-ray tube has been upgraded to state of the art **nanofocus 225 kVp**.

- X-ray source
  - 10 - 225 kV
  - **Focus spot < 0.8 µm**
- Detector
  - a-Si flat panel
  - 1210 x 1216 pixels
  - 0.1 x 0.1 mm^2
- Six-axis, high precision manipulator
- Magnification factor ≤ 2000

Gold foil spiral (foil thickness – 5 µm)

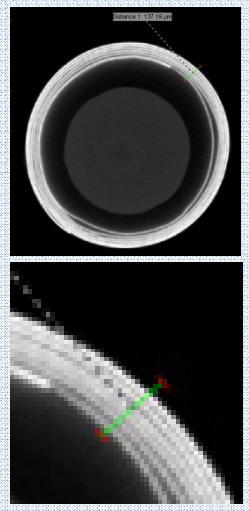

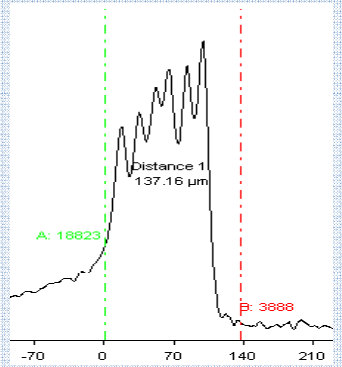

Micro Resolution Chart for X-ray 0.4-15 µm

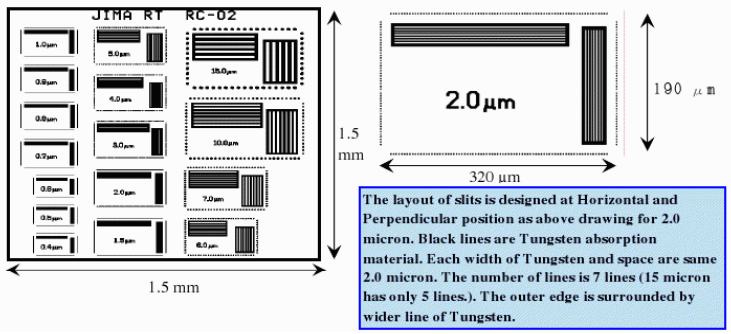

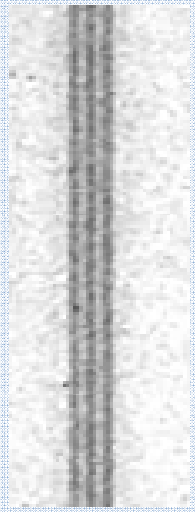

Resolution benchmark: JIMA Mask (< 0.4 µm)

X-ray transmission micro-tomography inspection of non-irradiated HFTM capsule

(designed and manufactured at FZK)

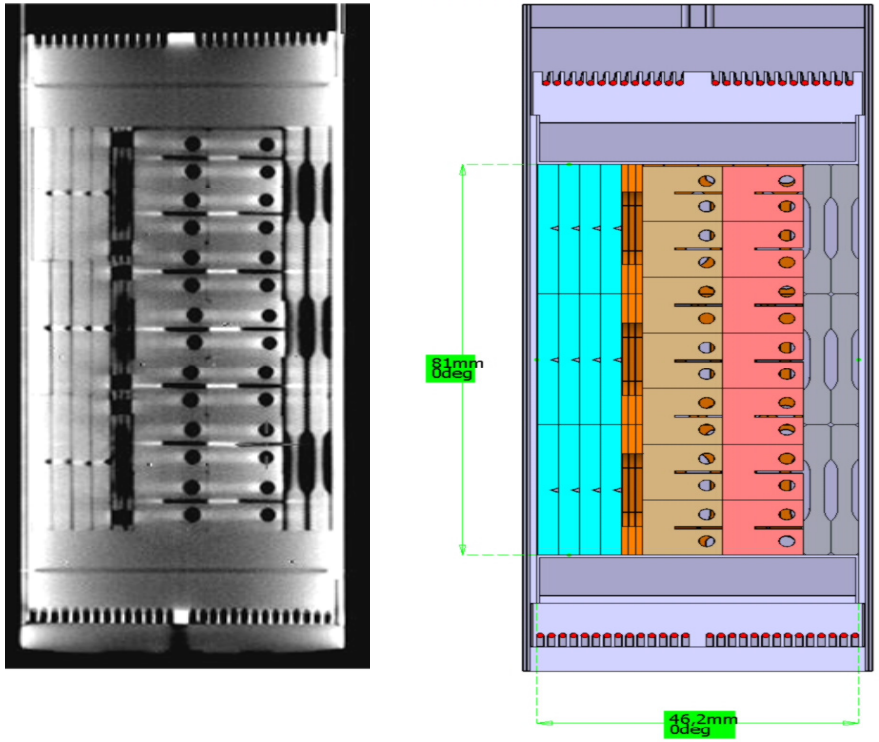

Cross-section through the X-ray microtomography reconstruction and corresponding picture of the irradiation capsule, shown as a CAD model

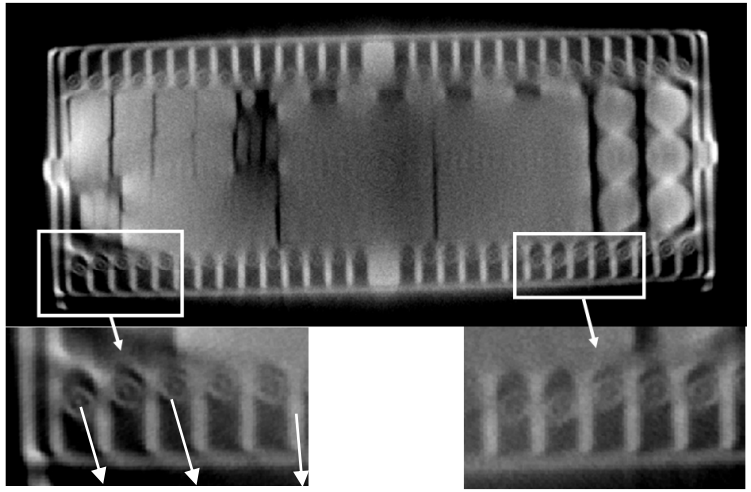

Tungsten wire Heater clad Groove

Tomographic cross-section illustrating the gap (lack of thermal contact) between the heater coil and the groove channel.

Details are clearly visible as, for example, the heater tube (1 mm diameter) with interior tungsten wire (100 μm diameter).

The absolute error of geometrical measurements is sufficient for the assessment of the structural integrity of the irradiation capsule and for the geometry description of the thermal-hydraulic modeling.

I. Tiseanu, M. Simon, T. Craciunescu, B. N. Mandache, Volker Heinzel, E. Stratmanns, S. P. Simakov, D. Leichtle. Assessment of the structural integrity of a prototypical instrumented IFMIF high flux test module rig by fully 3D X-ray microtomography. Fusion Engineering and Design, 82, p. 2608–2614, 2007.

Brazing quality assessment

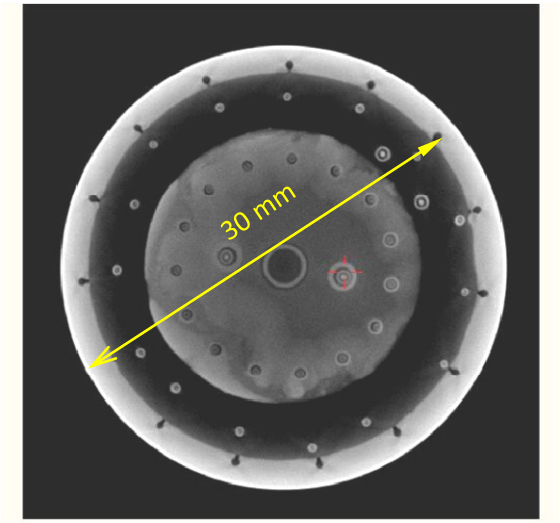

- samples with similar composition and even larger dimensions than the HFTM rig

- braze by nickel based filler metals used to high temperature base metals as in the HFTM rig.

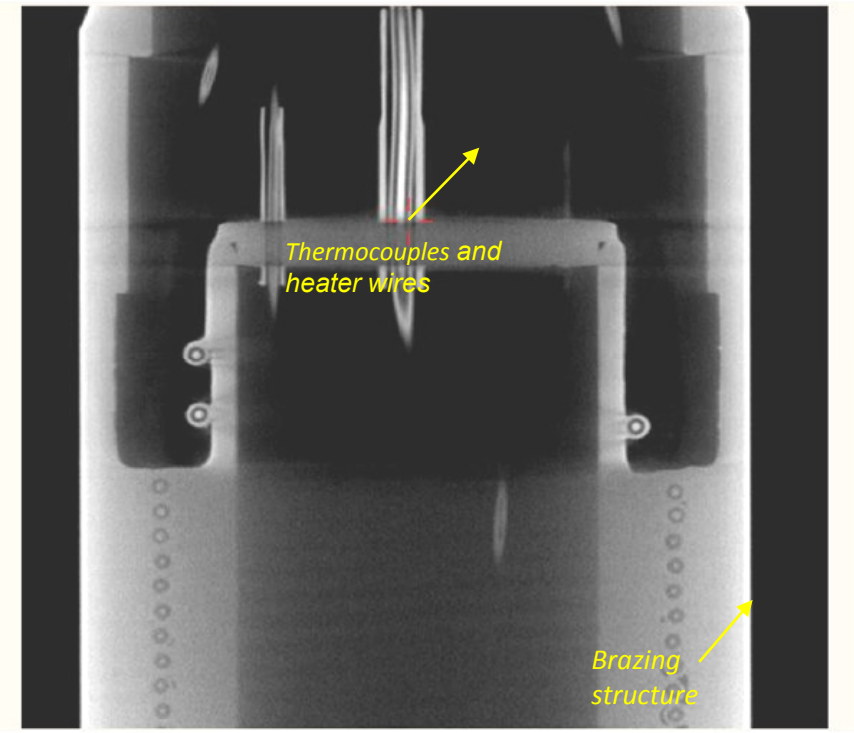

ITHEX experimental facility (FZK)

- dedicated to thermal-hydraulic investigations concerning mini-channel geometries as applied in IFMIF.

- several mini-channel test sections are investigated in order to optimize the HFTM helium cooling technology.

- the mini-channel test sections can be heated by electrical heaters and are instrumented with thermocouples to measure the temperature distribution.

WP10-PWI-01-02-01/MEdC/BS/PS

X-ray micro-tomography studies CFC samples for porosity network characterization

- Participation at DITS project - post mortem analysis by providing high resolution tomography measurements on CFC samples
- Qualification of the initial porosity of the new CFC ITER reference material NB41
- Porosity characterization of tungsten coated CFC samples

CFC Nb31: High resolution tomography

Sample size: ≥ 4x4x4 mm^3

Voxel resolution

14 μm

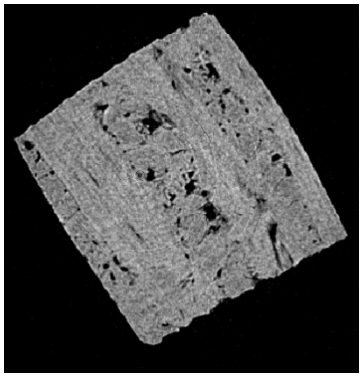

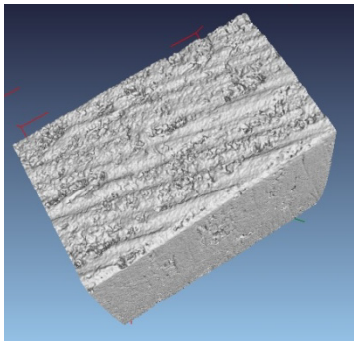

5 μm

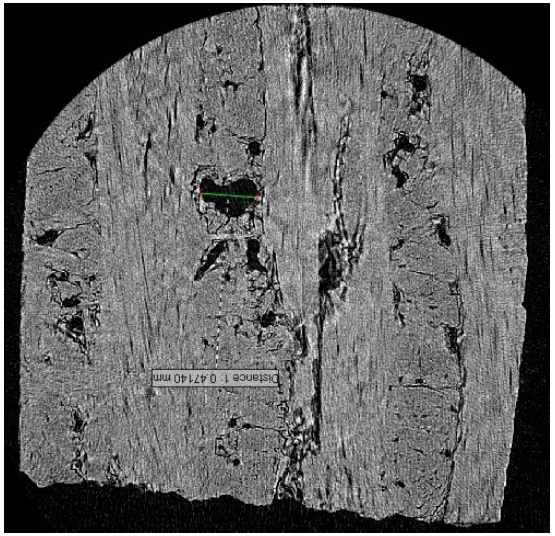

Offset tomography

2.5 μm

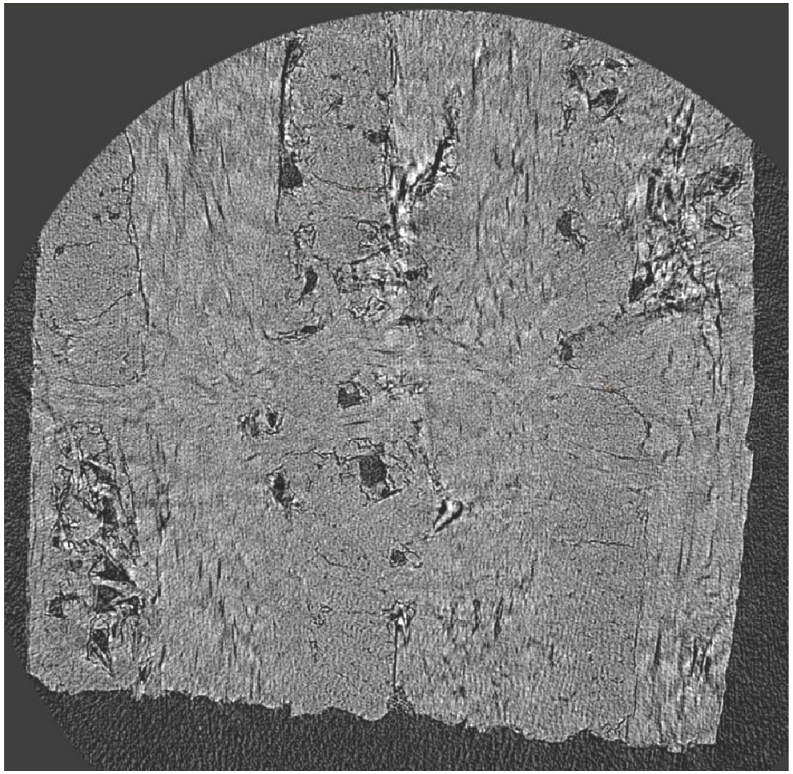

The main challenge is posed by the required micron range of the spatial resolution for rather macroscopic samples.

Quantitative evaluation of the CFC porosity factor

- A procedure for a quantitative evaluation of the sample porosity factor has been introduced and tested. For example for CFC NB31 and CFC DMS780 we obtained porosity factors of 8-10%.

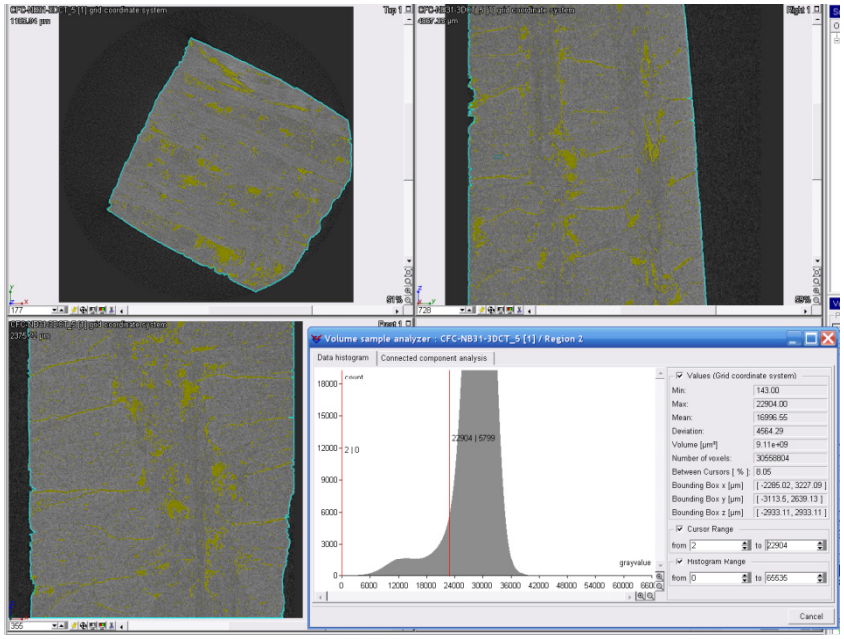

CFC NB31: 6 µm/voxel; porosity factor 8.05%

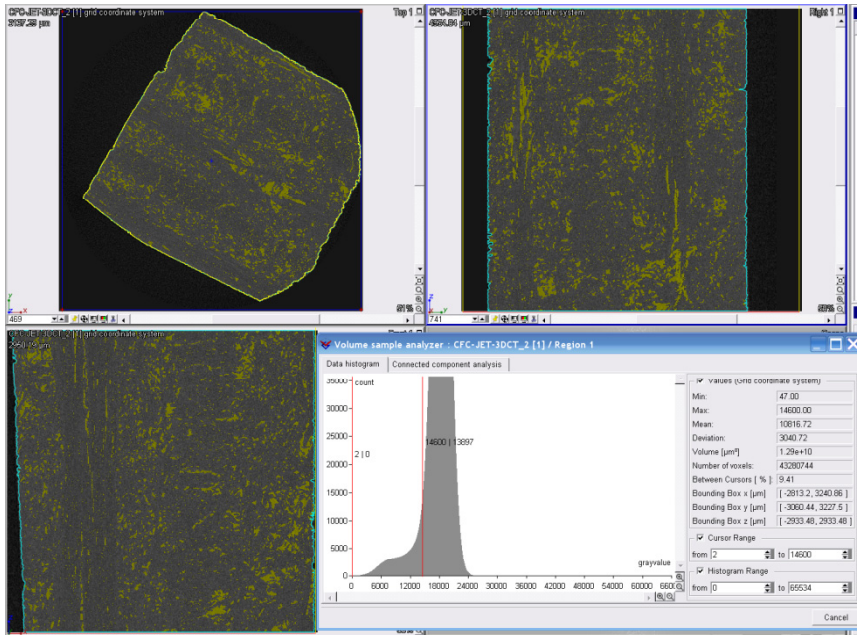

CFC DMS780: 6 µm/voxel; porosity factor 9.41%

Deuterium Inventory in Tore Supra (DITS) post mortem analysis
CFC-NB11

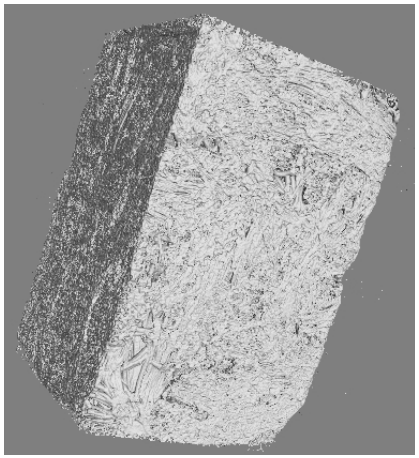

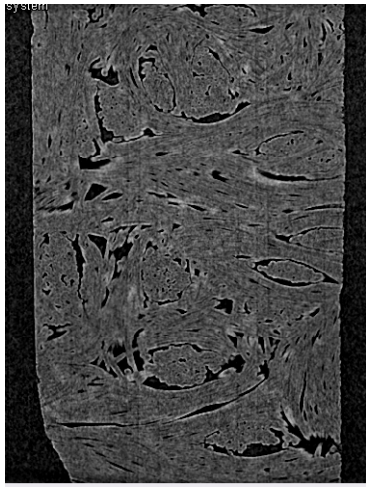

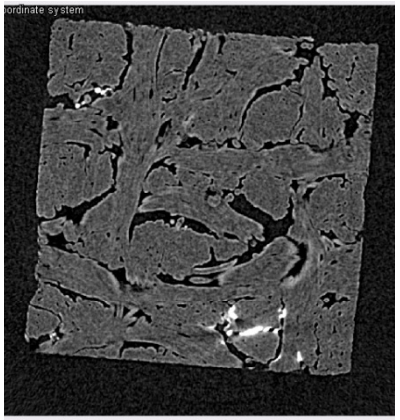

Voxel resolution ~ 2.8 μm

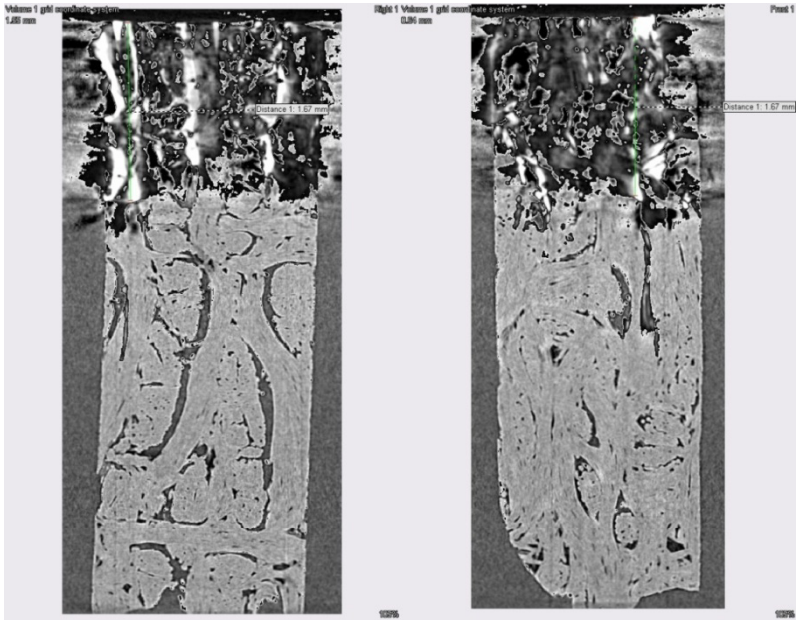

Cu brazed CFC NB11:
- pattern of Cu “filaments” along the fiber interspaces

Sample size: ≥ 2x2x5 mm^3

Deuterium Inventory in Tore Supra (DITS) post mortem analysis

- Quantitative evaluation of the CFC porosity factor

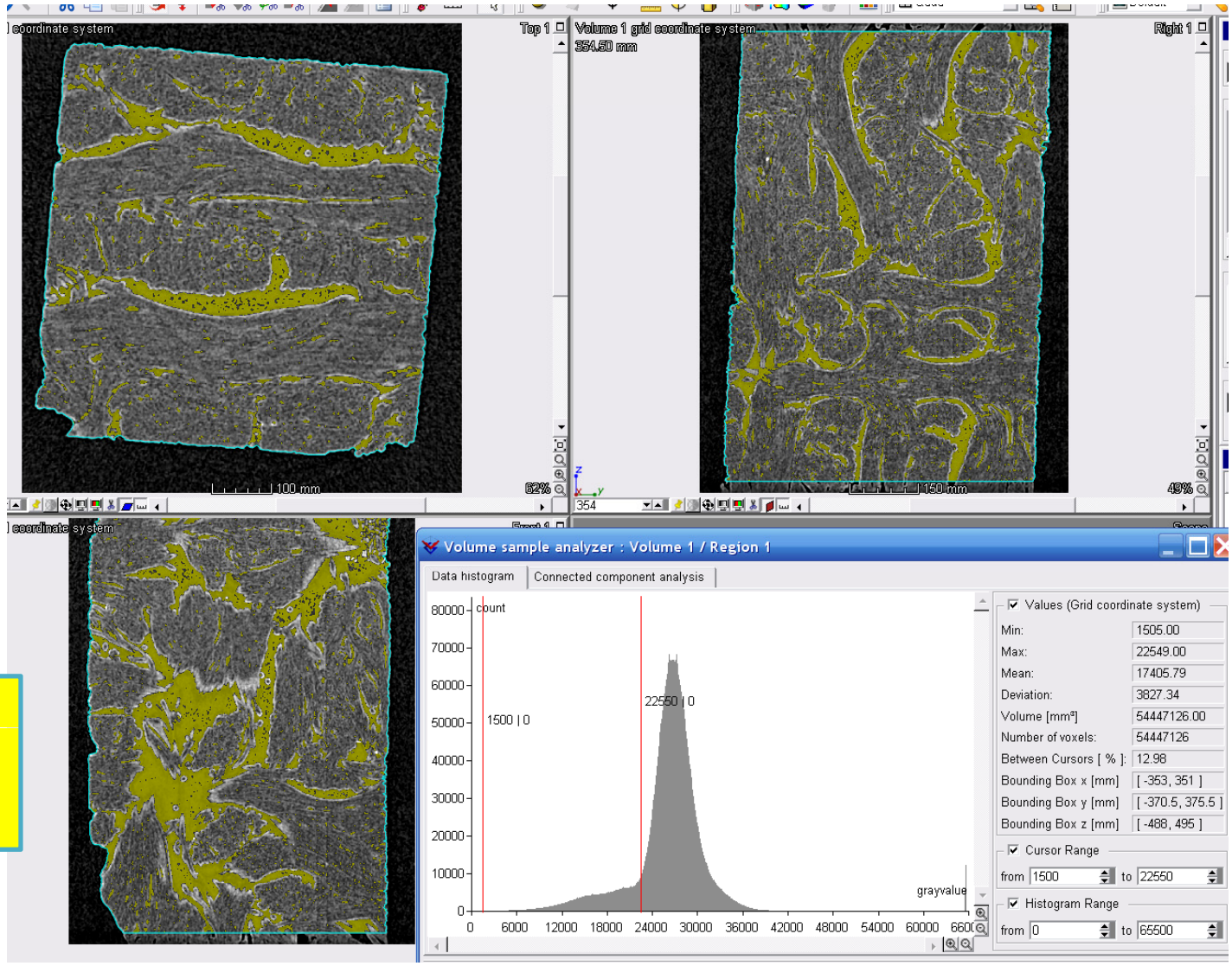

CFC NB11:
2.8 µm/voxel;
porosity factor
~13%

WP10-PWI-05-02-01/MEdC/BS/PS

X-ray microbeam absorption/fluorescence method as a non-invasive solution for investigation of the erosion of W coatings on graphite/CFC

- Quantitative evaluation of the thickness/uniformity/erosion/deposition of the tungsten coatings on graphite tiles from ASDEX Upgrade and of the tungsten coatings on ITER-like CFC tiles. Marker probes of Al C Ni W will be also measured.
- Comparison with previous quantitative analysis with EPMA, RBS and NRA.

Elaboration of a technical concept for a compact/low cost instrument based on X-ray micro-fluorescence to be used in high productivity coating analysis.

Tomo-Analytic

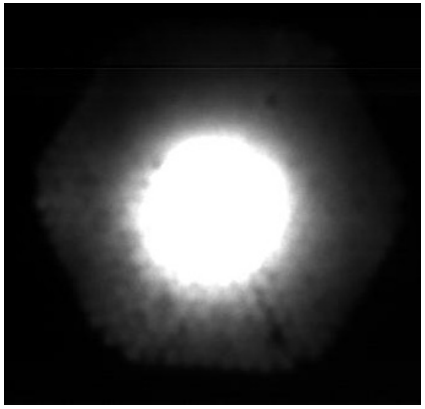

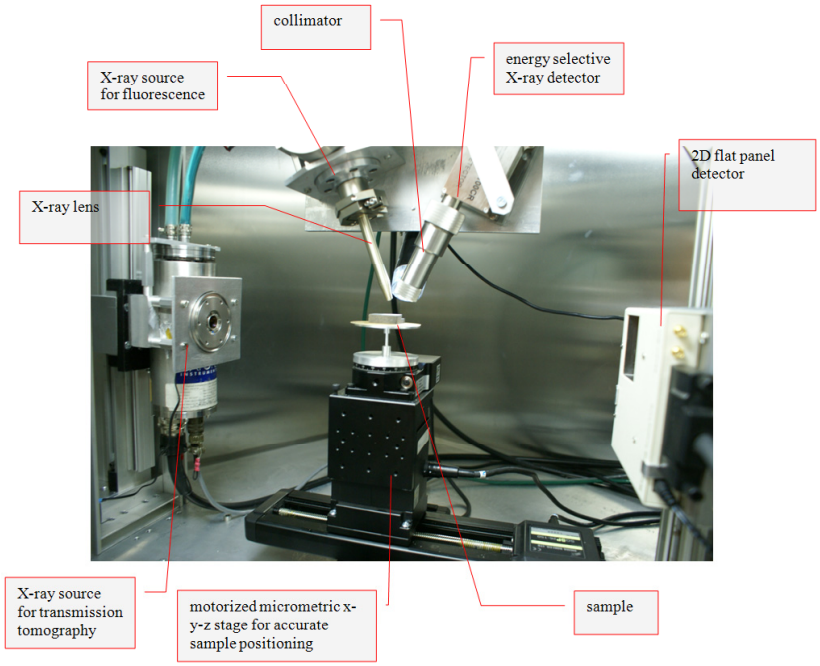

Computer tomography (µCT) systems are configured to take many views of the object in order to build a 3-D model of its internal structure. For the NDT inspection of miniaturised samples the microtomography analysis is guaranteed for feature recognition down to a few tens of microns. 3-D tomographic reconstructions are obtained by a proprietary highly optimized computer code based on a modified Feldkamp algorithm.

The microbeam fluorescence (µXRF) component is a configurable film thickness and composition measuring tool. Main components: optical X-ray beam collimation options, a PIN diode X-ray detector, motorized micrometric x-y-z stage for accurate sample positioning.

Combined X-ray absorption/fluorescence method for erosion analysis

Post-mortem analysis of fine graphite coating for ASDEX Upgrade tiles (divertor)

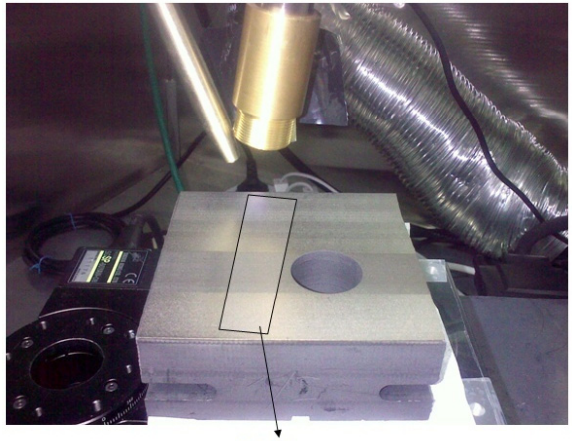

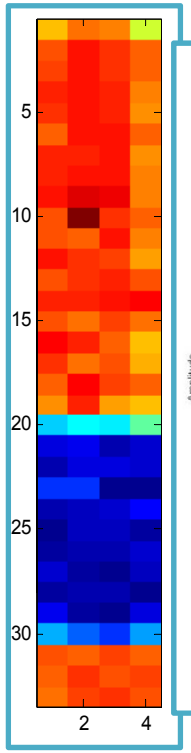

X-ray fluorescence spectra of W on fine graphite

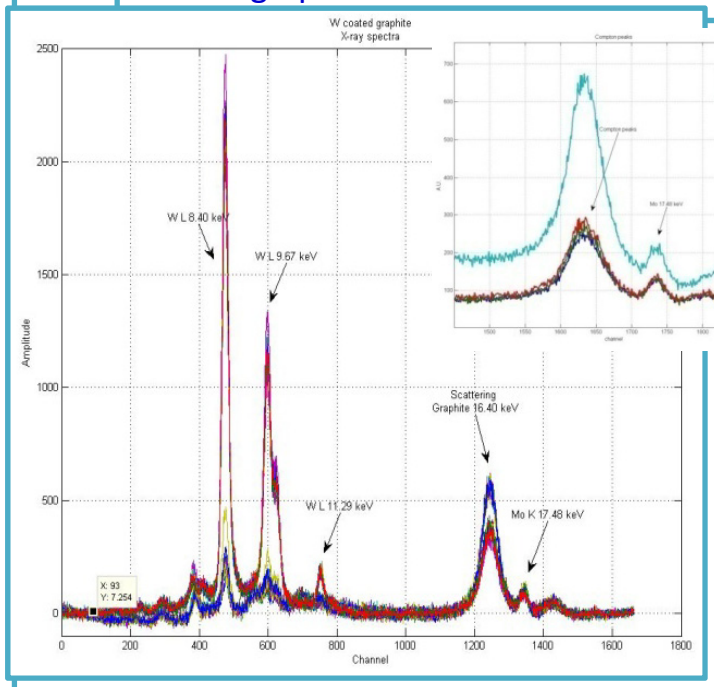

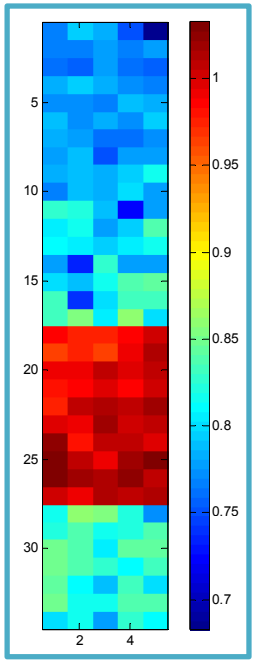

X-ray transmission map

The X-ray transmitted intensity was normalized to an average value of the transmission through the graphite. In this way we ignored the very low amount of redeposited W.

The red area corresponds the graphite stripe.

Map of the tungsten layer thickness and line profiles (scanning step: 2 mm)

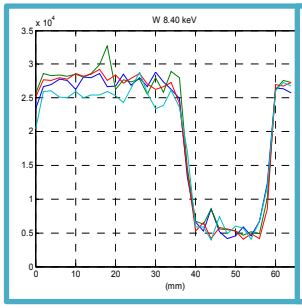

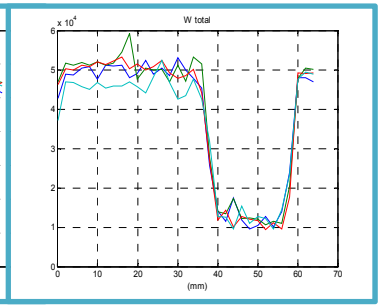

- the estimated lateral resolution: ~30 μm
- in-depth resolution: ~ 3% of the layer thickness.

Combined X-ray absorption/fluorescence method for erosion analysis

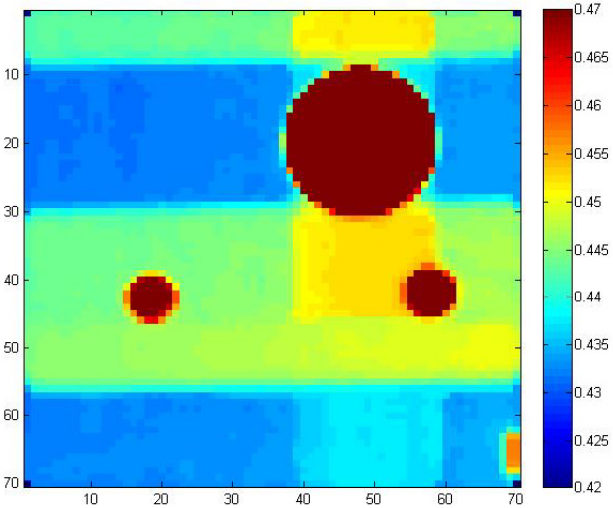

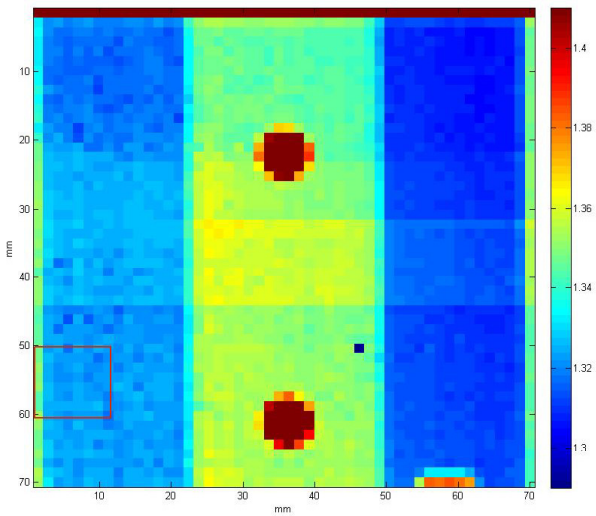

X-ray transmission map

The X-ray transmitted intensity was normalized to an average value of the transmission through the graphite. In this way we ignored the very low amount of redeposited W.

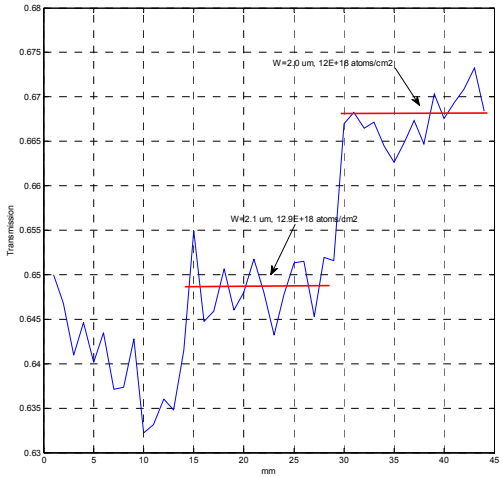

Calibration sample

Graphite tiles with W coating

NDT inspection of superconductors

- ITER Like Nb3Sn Superconductor
- EFDA HT SC - Mgb2
- Quality Control Monitoring of NbTi Strands and Conductor for JT-60SA TF Coils

X-ray microtomography on ITER type Nb3Sn superconductor wires

- inter-filament contacts
- twist-pitch parameter

Oxford Instruments (OST), for ITER
Type I, 0.81 mm (NbTi)3Sn strand, 19 subelements), Single Ta barrier,
Cu:non-Cu ratio 1

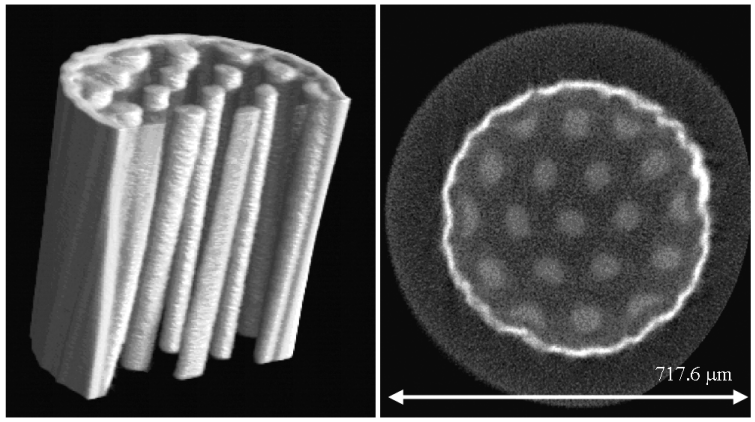

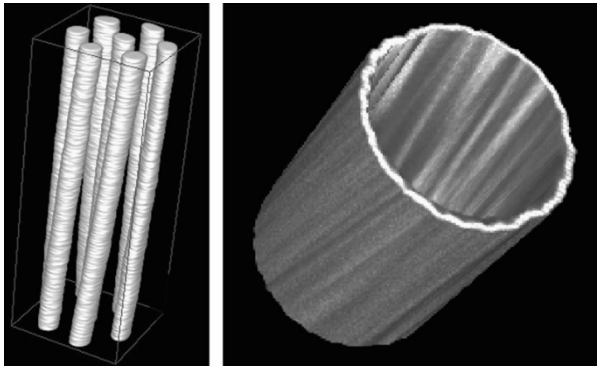

Extraction of the central filaments (left) and of the Ta sleeve (right).

Reconstruction evidencing the twisted structure

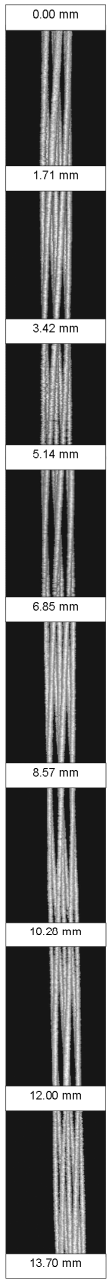

The traditional method for measuring the filamentary twist pitch arameter consists of:

- lamination
- etching the copper in a nitric acid solution

evidencing the twisted structure despite of the Ta barrier.

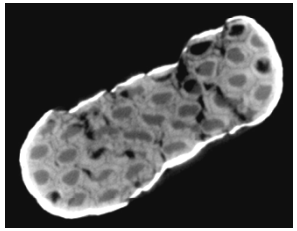

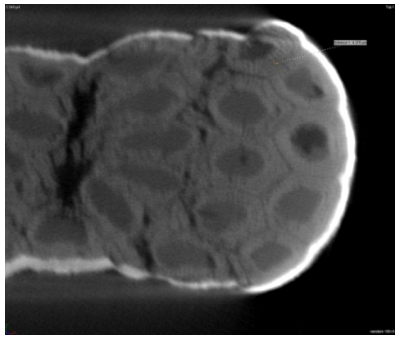

Enhanced resolution: 1.2 µ m

I. Tiseanu, T. Craciunescu, T. Petrisor, A. della Corte. 3D X-ray micro-tomography for modeling of NB3SN multifilamentary superconducting wires. Fusion Engineering and Design, 82, p. 1447–1453, 2007.

X-ray microtomography on MgB2 superconductor wires

- defects identification

X-ray microtomography images of the HYPERTECH MgB2 wires

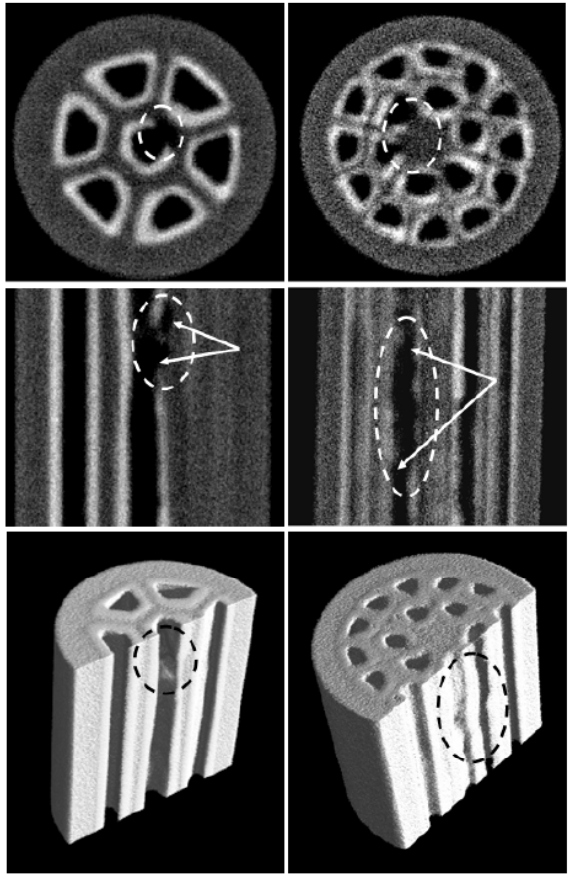

Tiseanu, T. Craciunescu, P. Badica, G. V. Aldica, M. Rindfleisch. Characterization of Superconducting Wires by Cone-Beam Micro-Tomography. In IEEE 2008 Workshop on X-Ray Micro Imaging of Materials, Devices, and Organisms, Nuclear Science Symposium Conference Record, 2008. NSS '08. IEEE, 2008. NSS '08. IEEE, pp. 582-585. 2008.

Structure and morphology of high density MgB2 superconductor

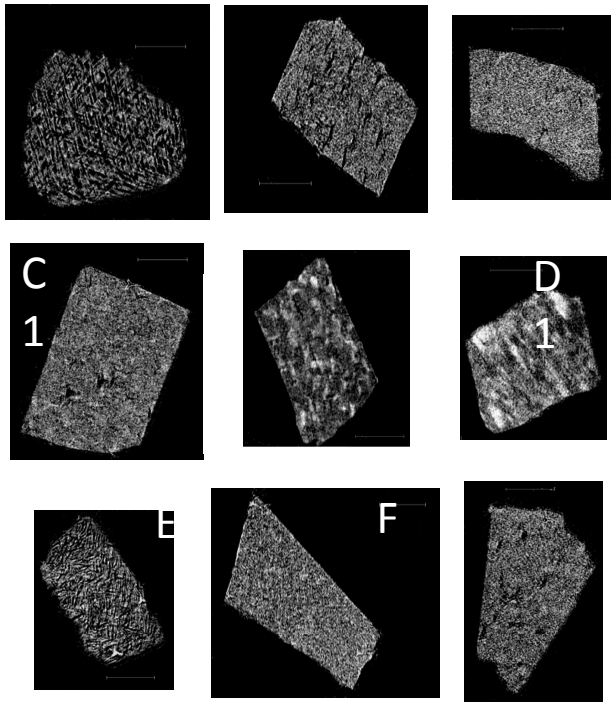

High density superconducting MgB2 is prepared using FAST (Field Assisted Sintering Technique) from very porous and mechanically weak mixture of Mg and B.

µCT can reveal clear differences between the samples helping the understanding of the milling-properties relationship (traditional techniques, like e.g. SEM proved to be insensitive)

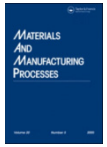

I. Tiseanu, T. Craciunescu, G. V. Aldica, M. Iovea. X-ray micro-tomography as a tool for quantitative characterization of advanced materials manufacturing processes. Advanced Materials Research, 47-50, pp. 698-701, 2008.

P Badica, G Aldica, T Craciunescu, I Tiseanu, Y Ma and K Togano. Microstructure of MgB2 samples observed by x-ray microtomography. Superconductor Science and Technology, 21, 2008.

TECHNICAL SPECIFICATION FOR QUALITY CONTROL MONITORING OF NBTI STRANDS AND CONDUCTOR FOR JT-60SA TF COILS: “EXTENDED GEOMETRY”

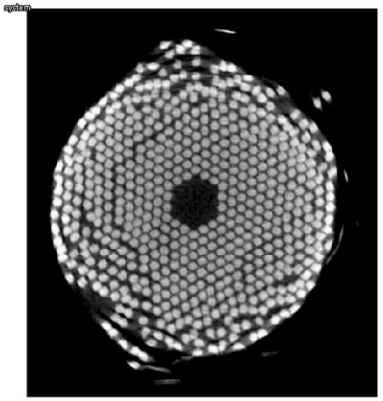

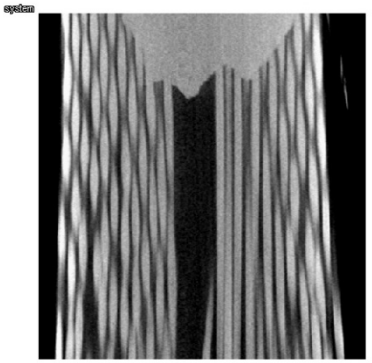

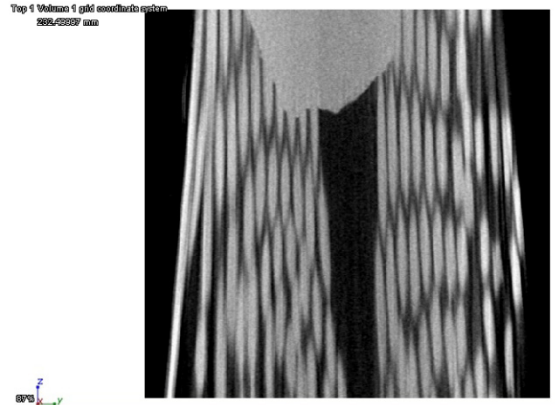

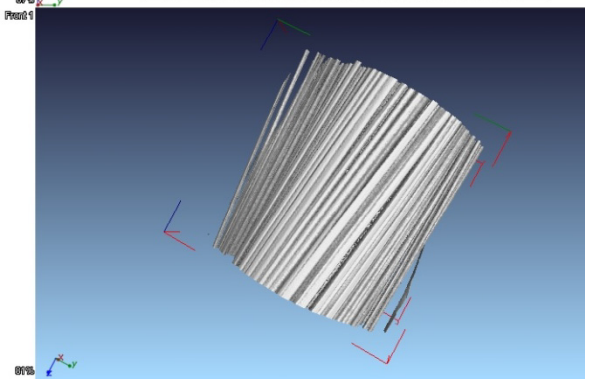

- a F4E-BA project -

NbTi strand tomographic examination in 3D configuration

#	Output data	Unit	Precision
1	Twist pitch average	mm	1 digit
2	Twist pitch standard deviation	mm	2 digits
3	Barrier average thickness	µm	1 digit
4	Barrier thickness standard deviation	µm	2 digits
5	Strand average volume for 1m of strand	mm^3	1 digit
6	Strand volume standard deviation for 1m of strand	mm^3	1 digit
7	SC average volume for 1m of strand	mm^3	1 digit
8	SC volume standard deviation for 1m of strand	mm^3	1 digit

3D tomography measurements on cable and soldered junctions between superconducting cables

Application: JT60SA a F4E-BA project

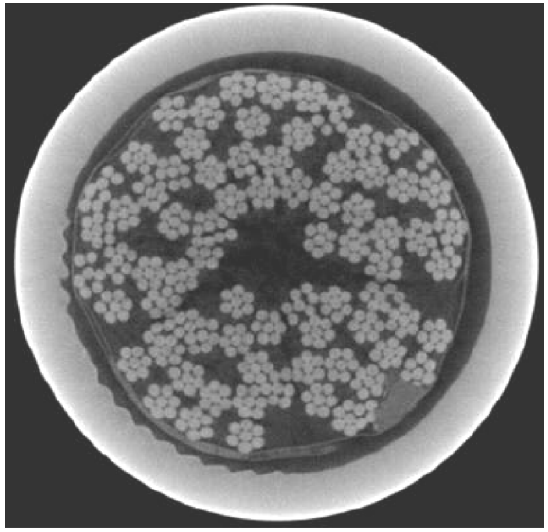

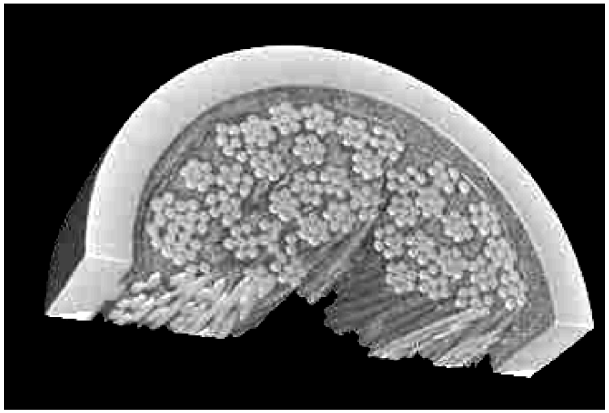

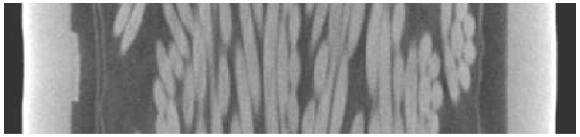

CT technique is able to detect a flow size well under 10% of the wall thickness of the cable stainless steel jacket (see images bellow). Based on this result we propose that microCT should be employed in the development and manufacturing of superconducting cables.
Thus one can provide strand trajectories map of a conductor sample on at least one twist pitch (cca. 300 mm) in order to check the void homogeneity during production.

#	Output data	Unit	Precision
1	Void fraction average	%	1 digit
2	Void fraction standard deviation	%	2 digits
3	Void homogeneity factor	adimensional	2 digits
4	Cos teta	adimensional	3 digits
5	Strand trajectories	$[mm]^3$	1 digit
6	Interstrand contacts linear density	m^{-1}	1 digit